

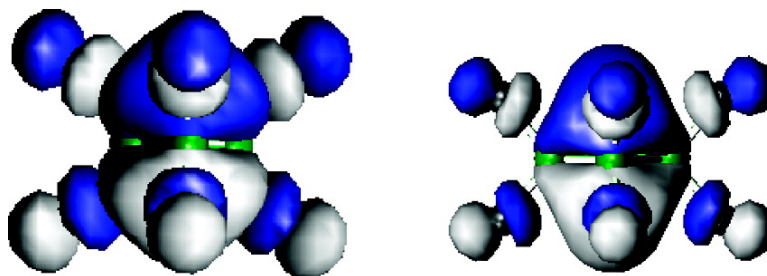
Article

**Computational and ESR Studies of Electron Attachment to Decafluorocyclopentane, Octafluorocyclobutane, and Hexafluorocyclopropane: Electron Affinities of the Molecules and the Structures of Their Stable Negative Ions as Determined from C and F Hyperfine Coupling Constants**

Adel M. ElSohly, Gregory S. Tschumper, Richard A. Crocombe, Jih Tzong Wang, and Ffrancon Williams

*J. Am. Chem. Soc.*, **2005**, 127 (30), 10573-10583 • DOI: 10.1021/ja0505898 • Publication Date (Web): 08 July 2005

Downloaded from <http://pubs.acs.org> on March 25, 2009



**More About This Article**

Additional resources and features associated with this article are available within the HTML version:

- Supporting Information
- Links to the 5 articles that cite this article, as of the time of this article download
- Access to high resolution figures
- Links to articles and content related to this article
- Copyright permission to reproduce figures and/or text from this article

[View the Full Text HTML](#)



**ACS Publications**  
High quality. High impact.

# Computational and ESR Studies of Electron Attachment to Decafluorocyclopentane, Octafluorocyclobutane, and Hexafluorocyclopropane: Electron Affinities of the Molecules and the Structures of Their Stable Negative Ions as Determined from $^{13}\text{C}$ and $^{19}\text{F}$ Hyperfine Coupling Constants

Adel M. ElSohly,<sup>†</sup> Gregory S. Tschumper,<sup>\*,†</sup> Richard A. Crocombe,<sup>\*,‡,§</sup>  
Jih Tzong Wang,<sup>‡</sup> and Ffrancon Williams<sup>\*,†</sup>

Contribution from the Department of Chemistry and Biochemistry, The University of Mississippi, University, Mississippi 38677, and the Department of Chemistry, The University of Tennessee, Knoxville, Tennessee 37996

Received January 28, 2005; E-mail: tschumpr@olemiss.edu; rcrocombe@axsun.com; williams@ion.chem.utk.edu

**Abstract:** High-resolution ESR spectra of the ground-state negative ions of hexafluorocyclopropane ( $c\text{-C}_3\text{F}_6^-$ ), octafluorocyclobutane ( $c\text{-C}_4\text{F}_8^-$ ), and decafluorocyclopentane ( $c\text{-C}_5\text{F}_{10}^-$ ) are reported and their isotropic  $^{19}\text{F}$  hyperfine coupling constants (hfcc) of  $198.6 \pm 0.4$  G,  $147.6 \pm 0.4$  G, and  $117.9 \pm 0.4$  G, respectively, are in inverse ratio to the total number of fluorine atoms per anion. Together with the small value of  $5.2 \pm 0.4$  G determined for the isotropic  $^{13}\text{C}$  hfcc of  $c\text{-C}_4\text{F}_8^-$ , these results indicate that in each case the singly occupied molecular orbital (SOMO) is delocalized over the equivalent fluorines and possesses a nodal plane through the carbon atoms of a time-averaged  $D_{nh}$  structure. A series of quantum chemical computations were carried out to further characterize these anions and their neutral counterparts. Both the B3LYP density functional and second-order Møller–Plesset perturbation theory (MP2) indicate that  $c\text{-C}_3\text{F}_6^-$  adopts a  $D_{3h}$  geometry and a  $^2A_2''$  ground electronic state, that  $c\text{-C}_4\text{F}_8^-$  adopts a  $D_{4h}$  geometry and a  $^2A_{2u}$  ground electronic state, and that  $c\text{-C}_5\text{F}_{10}^-$  adopts a  $C_s$  structure and a  $^2A'$  electronic state. Moreover, the  $^{19}\text{F}$  hyperfine coupling constants computed with the MP2 method and a high quality triple- $\zeta$  basis set are within 1% of the experimental values. Also, the values computed for the  $^{13}\text{C}$  hfcc of  $c\text{-C}_4\text{F}_8^-$  are consistent with the experimental value of 5.2 G. Therefore, in keeping with the ESR results, these negative ions derived from first-row elements can be characterized as  $\pi^*$  species. In addition, the hypervalency of these perfluorocycloalkane radical anions has been clarified.

## 1. Introduction

Electron interactions with perfluorocycloalkanes ( $c\text{-C}_n\text{F}_{2n}$  for  $n = 3\text{--}6$ ) are of both practical and fundamental interest. The practical importance stems, in large part, from the use of these compounds in low-temperature gaseous plasmas that have found particular application for the manufacture of integrated circuits in the solid-state microelectronics industry.<sup>1–3</sup> For example, in the fabrication of semiconductor components, octafluorocyclobutane ( $c\text{-C}_4\text{F}_8$ ) is used as the plasma feed gas to achieve high selectivity in the etching of silicon dioxide over silicon, a critical step in the overall process.<sup>4,5</sup> Evidently, the physics and chemistry of the elementary reactions brought about by electron

excitation and capture in these etchant gases are relevant to the practice of this modern technology.<sup>6,7</sup>

In particular, numerous gas-phase studies<sup>8–21</sup> have shown that electron attachment to  $c\text{-C}_4\text{F}_8$  can occur nondissociatively for incident electrons in the energy range from ca. 0.5 eV down to the thermal values associated with the Boltzmann distribution

<sup>†</sup> The University of Mississippi.

<sup>‡</sup> The University of Tennessee.

<sup>§</sup> Present address: Axsun Technologies, 1 Fortune Drive, Billerica, MA 01821.

- (1) Lieberman, M. A.; Lichtenberg, A. J. *Principles of Plasma Discharge and Materials Processing*; Wiley: New York, 1994.
- (2) Tachi, S. *J. Vac. Sci. Technol.* **2003**, *A21*, S131.
- (3) Teii, S.; Hori, M.; Ito, M.; Goto, T.; Ishii, N. *J. Vac. Sci. Technol.* **2000**, *A18*, 1.
- (4) Jung, C. O.; Chi, K. K.; Hwang, B. G.; Moon, J. T.; Lee, M. Y.; Lee, J. G. *Thin Solid Films* **1999**, *341*, 112.
- (5) Hopwood, J.; Mantei, T. D. *J. Vac. Sci. Technol.* **2003**, *A21*, S139.

- (6) Winstead, C.; McKoy, V. *AIP Conference Proceedings* **2002**, *636*, 241.
- (7) Winstead, C.; McKoy, V. *J. Chem. Phys.* **2001**, *114*, 7407.
- (8) Chutjian, A.; Alajajian, S. H. *J. Phys. B* **1987**, *20*, 839.
- (9) Morris, R. A.; Miller, T. M.; Viggiano, A. A.; Paulson, J. F.; Solomon, S.; Reid, G. *J. Geophys. Res. [Atmos]* **1995**, *100*, 1287.
- (10) Miller, T. M.; Friedman, J. F.; Viggiano, A. A. *J. Chem. Phys.* **2004**, *120*, 7024.
- (11) Hirakoa, K.; Mizuno, T.; Eguchi, D.; Takao, K.; Iino, T.; Yanabe, S. *J. Chem. Phys.* **2002**, *116*, 7574.
- (12) Christophorou, L. G.; Olthoff, J. K. *J. Phys. Chem. Ref. Data* **2001**, *30*, 449.
- (13) Jiao, C. Q.; Garscadden, A.; Haaland, P. D. *Chem. Phys. Lett.* **1998**, *297*, 121.
- (14) Bibby, M. M.; Carter, G. *Trans. Faraday Soc.* **1963**, *59*, 2455.
- (15) Naff, W. T.; Cooper, C. D.; Compton, R. N. *J. Chem. Phys.* **1968**, *49*, 2784.
- (16) Davis, F. J.; Compton, R. N.; Nelson, D. R. *J. Chem. Phys.* **1973**, *59*, 2324.
- (17) Christophorou, L. G.; McCorkle, D. L.; Pittman, D. J. *J. Chem. Phys.* **1974**, *60*, 1183.
- (18) Bansal, K. M.; Fessenden, R. W. *J. Chem. Phys.* **1973**, *59*, 1760.
- (19) Fessenden, R. W.; Bansal, K. M. *J. Chem. Phys.* **1970**, *53*, 3468.
- (20) Harland, P. W.; Thynne, J. C. *Int. J. Mass Spectrom. Ion Phys.* **1973**, *10*, 11.
- (21) Lifschitz, C.; Grajower, R. *Int. J. Mass Spectrom. Ion Phys.* **1973**, *10*, 25.

that applies for electron "swarms". Such  $c\text{-C}_4\text{F}_8$  ions are considered to be metastable with respect to the reverse process of electron detachment and to have typical lifetimes in the region of about 10  $\mu\text{s}$ .<sup>15,20</sup> Indeed, the excellent dielectric properties of  $c\text{-C}_4\text{F}_8$  and its use as a high-voltage insulator can be attributed to this singular step for ensuring efficient energy transfer from epithermal electrons to the  $c\text{-C}_4\text{F}_8$  molecules with no resultant chemical change. At energies above 1.75 eV, however, electron attachment is said to be dissociative with the fragment ion being  $\text{F}^-$ ,  $\text{C}_3\text{F}_5^-$ ,  $\text{C}_2\text{F}_5^-$ ,  $\text{CF}_3^-$ ,  $\text{C}_2\text{F}_3^-$ , or  $\text{CF}_2^{\bullet-}$ , depending on the resonant energy acquired by the negative-ion state in the collision.<sup>12</sup> Such reactions are of particular interest with respect to physical and chemical processes in the upper atmosphere.<sup>9</sup>

Considerable effort has, therefore, been expended on understanding the physics of these molecular ionization and attachment processes, and a main focus has been the accumulation of cross-section data for the interactions of fluorocompounds and other potential etchant gases with the low-energy electrons (ca. 1–10 eV) that are typically present in the plasmas.<sup>6,12</sup> On the other hand, some basic chemical issues are also involved, a key question being the structural nature of electron attachment to a closed-shell saturated  $c\text{-C}_n\text{F}_{2n}$  molecule and its chemical consequences.<sup>22</sup> Since these molecules contain no well-defined chromophores that could act as *localized* sites for electron capture, the detailed structure of the negative ion is not immediately obvious, and gas-phase studies have contributed little in the way of structural detail. Indeed, some early speculation<sup>23</sup> centered on the notion that such molecules could only provide "intramolecular electrostatic traps" for electrons. Also, it is useful to consider from a chemical standpoint the factors that are likely to determine the stability of the parent negative ion with respect to either electron loss or chemical dissociation,<sup>24</sup> especially since the latter process can conceivably give rise to either a fluoride or other fragment anion.

Previous ESR spectroscopic studies<sup>25,26</sup> have been carried out on  $\gamma$ -irradiated and photoionized solid solutions of these  $c\text{-C}_n\text{F}_{2n}$  compounds in neopentane and tetramethylsilane. These solid matrixes possess rotator phases that give rise to nearly isotropic ESR spectra of the perfluorocycloalkane radical anions formed by irradiation. Thus, it was established that perfluorocycloalkanes also undergo electron capture in the condensed phase to form negative ions<sup>27</sup> with characteristic  $^{19}\text{F}$  hyperfine signatures corresponding to a complete set of equivalent fluorines for each radical anion. Furthermore, the inverse dependence of the  $^{19}\text{F}$  hyperfine coupling on the  $c\text{-C}_n\text{F}_{2n}$  ring size ( $n = 3\text{--}5$ ) pointed unambiguously to the delocalization of

the odd electron in an unusual antibonding type of singly occupied molecular orbital,<sup>28</sup> and this interpretation was certainly in line with the well-known tendency of the  $\text{C}\text{--}\text{F}$   $\sigma^*$  orbitals to act as electron acceptors.<sup>7,29–31</sup> However, a definitive assignment as to the actual ground state of the particular negative ion could not be made because the low spectral resolution was unable to provide information on the structurally diagnostic  $^{13}\text{C}$  hyperfine coupling constants. Moreover, the prevailing INDO and other semiempirical calculations of the 1970s lacked sufficient precision to discriminate between the alternate negative ion states on the basis of either energy differences or predicted  $^{19}\text{F}$  hyperfine couplings.

The present paper reports density functional and ab initio computations as well as ESR studies that shed new light on the ground-state structures of  $c\text{-C}_n\text{F}_{2n}$  molecules and their negative ions for  $n = 3\text{--}5$ . First, in addition to obtaining the adiabatic electron affinities of the parent molecules, the  $^{19}\text{F}$  and  $^{13}\text{C}$  hyperfine coupling constants have been calculated for the ground states of the negative ions using four different basis sets. Second, new high-resolution ESR spectra of the negative ions are presented. As a result, through the generation of the fully  $^{13}\text{C}$ -labeled  $c\text{-C}_4\text{F}_8^{\bullet-}$ , the  $^{13}\text{C}$  hyperfine splitting has been observed together with the full higher-order structure associated with the presence of large  $^{19}\text{F}$  coupling constants.<sup>25,26,32–36</sup> From these results, a comparison of the measured hyperfine couplings with the values predicted by the theoretical calculations allows definitive structural assignments of the  $c\text{-C}_n\text{F}_{2n}$  negative ions to be made for the first time.

## 2. Experimental Methods

Octafluorocyclobutane (Freon C 318) was obtained from Peninsular Chem Research (PCR, Inc.) and from Air Products and Chemicals, Inc. Assays in each case performed by gas-chromatographic analysis showed a purity exceeding 99%, and the  $\gamma$ -irradiated  $c\text{-C}_4\text{F}_8$  solid solutions (see below) prepared from either of these two sources gave identical ESR results. A sample of hexafluorocyclopropane was kindly donated to us by Dr. R. W. Fessenden from material that was originally prepared by Dr. K. Hartman.<sup>18</sup> Decafluorocyclopentane and tetrafluoroethylene were supplied by PCR, Inc. Hexamethylethane (HME), also known as 2,2,3,3-tetramethylbutane, from the Aldrich Chemical Co., Inc. was used exclusively as the solvent matrix throughout this work. Previous work showing that intense isotropic ESR spectra of  $\text{C}_6\text{F}_6^{\bullet-}$  are observed from  $\gamma$ -irradiated solutions of hexafluorobenzene<sup>37</sup> in HME at 174 K suggested the use of this matrix in the present study.

(22) Of historical interest is a claim to have observed the ESR spectrum of the cyclopropane- $h_6$  radical anion in solution (Bowers, K. W.; Greene, F. D. *J. Am. Chem. Soc.* **1963**, *85*, 2331). However, the observation could not be repeated (Gerson, F.; Heilbronner, E.; Heinzer, J. *Tetrahedron Lett.* **1966**, *7*, 2095), and the claim was retracted (Bowers, K. W.; Nolfi, Jr., G. J.; Lowry, T. H.; Greene, F. D. *Tetrahedron Lett.* **1966**, *7*, 4063). Other ESR reports of radical anion formation by closed-shell saturated hydrocarbons such as adamantane in solution have also not been confirmed, and such results have been attributed to electron capture by traces of impurities such as benzene (Jones, M. T. *J. Am. Chem. Soc.* **1966**, *88*, 174).

(23) Mittal, J. P.; Libby, W. F. *Nature* **1968**, *220*, 1027.

(24) Sprague, E. D.; Williams, F. *J. Chem. Phys.* **1971**, *54*, 5425.

(25) Shiotani, M.; Williams, F. *J. Am. Chem. Soc.* **1976**, *98*, 4006.

(26) Hasegawa, A.; Shiotani, M.; Williams, F. *Faraday Discussions Chem. Soc.* **1977**, *63*, 157.

(27) The electrochemical reduction potentials of the  $c\text{-C}_n\text{F}_{2n}$  perfluorocycloalkanes do not appear to have been determined. For recent studies by cyclic voltammetry on the reduction of other perfluorocarbons, including perfluorodecalin, see: (a) Combellas, C.; Kanoufi, F.; Thiebault, A. *J. Phys. Chem. B* **2003**, *107*, 10894. (b) Pud, A. A.; Shapoval, G. S.; Kukhar, V. P.; Mikulina, O. E.; Gervits, L. L. *Electrochim. Acta* **1995**, *40*, 1157.

(28) A recent theoretical paper (Gallup, G. A. *Chem. Phys. Lett.* **2004**, *399*, 206) notes the highly unusual nature of these perfluorocycloalkane radical anions by remarking that, for  $c\text{-C}_4\text{F}_8$ , "it is perhaps surprising that such a relatively small saturated molecule, made entirely of elements from the second row of the periodic table, possesses a stable negative ion". As far as we are aware, the only other closed-shell molecule of this kind that forms a negative ion in solution is  $\text{F}_3\text{NO}$  (Nishikida, K.; Williams, F. *J. Am. Chem. Soc.* **1975**, *97*, 2331. Hasegawa, A.; Hudson, R. L.; Kikuchi, O.; Nishikida, K.; Williams, F. *J. Am. Chem. Soc.* **1981**, *103*, 3436). This exclusiveness is further illustrated by the fact that the negative ion of the isoelectronic  $\text{CF}_4$  molecule is unknown, at least in solution. Similarly, the negative ions of the higher perfluoro- $n$ -alkanes have not been observed, although theoretical calculations point to positive adiabatic electron affinities except in the case of  $\text{C}_2\text{F}_6$  (Paul, A.; Wannere, C. S.; Schaefer, H. F. *J. Phys. Chem. A* **2004**, *108*, 9428).

(29) Liebman, J. F. *J. Fluorine Chem.* **1973/1974**, *3*, 27.

(30) Ishii, I.; McLaren, R.; Hitchcock, A. P.; Jordan, K.; Choi, Y.; Robin, M. B. *Can. J. Chem.* **1988**, *66*, 2104.

(31) Borden, W. T. *Chem. Commun.* **1998**, 1919.

(32) Fessenden, R. W. *J. Chem. Phys.* **1962**, *37*, 747.

(33) Fessenden, R. W.; Schuler, R. H. *J. Chem. Phys.* **1965**, *43*, 2704.

(34) Kerr, C. M. L.; Webster, K.; Williams, F. *J. Phys. Chem.* **1975**, *79*, 2650.

(35) Hasegawa, A.; Hayashi, M.; Kerr, C. M.; Williams, F. *J. Magn. Reson.* **1982**, *48*, 192.

(36) Fessenden, R. W. *J. Magn. Reson.* **1969**, *1*, 277.

(37) Wang, J. T.; Williams, F. *Chem. Phys. Lett.* **1980**, *71*, 471.

Solid solutions typically containing 1–4 mol % of the perfluoro-carbon in HME were prepared in 4 mm o.d. spectroil tubes on a vacuum line by transfer of the volatile components from storage reservoirs. After the sample tube had been sealed off, it was heated above the melting point of HME (101 °C) to allow for thorough mixing of the two components and then cooled rapidly by transfer to a water bath at room temperature. This procedure ensured that the solid material was retained in the lower part of the tube corresponding to its placement in the most sensitive region of the ESR spectrometer cavity. The sample tubes were exposed to total doses of 0.6 to 1.0 Mrad (1 Mrad =  $1 \times 10^4$  J kg<sup>-1</sup> = 10 kGy) at 77 K in a cobalt-60 irradiator (Gammacell 200 from Atomic Energy of Canada, Ltd.).

ESR measurements were carried out at variable temperatures in the range from 80 to 170 K as described previously<sup>26,38,39</sup> using either the Bruker ER 200D SRC or Varian V-4502-15 spectrometers. Magnetic field strengths were determined using proton NMR gaussmeters (Bruker model 035M or the Walker/Magnetronics model G-502), and the X-band microwave frequency was monitored by either the Systron-Donner 6054B or the 1037 counter. The large <sup>19</sup>F coupling constants were calculated from the spectral line positions using the higher-order solutions<sup>32–36</sup> of the appropriate spin Hamiltonian.

For diagnostic purposes explained in the Introduction, a key objective of this work was to determine the isotropic <sup>13</sup>C hyperfine splitting in these perfluorocycloalkane negative ions. Since this splitting could not be observed even in intense ESR spectra from *c*-C<sub>n</sub>F<sub>2n</sub><sup>•-</sup> species with the <sup>13</sup>C present in natural abundance, it was desirable to obtain spectra from <sup>13</sup>C-labeled negative ions. A direct approach to this goal through the use of a fully <sup>13</sup>C-labeled perfluorocycloalkane would have presented a formidable synthetic problem. However, a circuitous but more practical method of achieving the same objective was opened up by the observation that  $\gamma$ -irradiated samples of tetrafluoroethylene in hexamethylethane (HME) gave much stronger *isotropic* ESR signals from *c*-C<sub>4</sub>F<sub>8</sub><sup>•-</sup> than from C<sub>2</sub>F<sub>4</sub><sup>•-</sup>. This result was not entirely unexpected for two reasons. First, weak signals from *c*-C<sub>4</sub>F<sub>8</sub><sup>•-</sup> had previously been noticed along with the isotropic spectrum of C<sub>2</sub>F<sub>4</sub><sup>•-</sup> from  $\gamma$ -irradiated solutions of C<sub>2</sub>F<sub>4</sub> in tetramethylsilane.<sup>40</sup> Second, evidence that a bimolecular reaction of C<sub>2</sub>F<sub>4</sub><sup>•-</sup> with C<sub>2</sub>F<sub>4</sub> to form *c*-C<sub>4</sub>F<sub>8</sub><sup>•-</sup> could occur with high efficiency under suitable matrix conditions was clearly indicated by the complete transformation of the anisotropic spectrum of C<sub>2</sub>F<sub>4</sub><sup>•-</sup> to that of *c*-C<sub>4</sub>F<sub>8</sub><sup>•-</sup> on annealing  $\gamma$ -irradiated samples of C<sub>2</sub>F<sub>4</sub> in methyltetrahydrofuran (MTHF).<sup>41,42</sup> Evidently, the HME matrix nicely fulfilled the twin requirements of allowing this ion–molecule reaction to occur while at the same time giving rise to isotropic ESR spectra. Thus, the problem was reduced to that of preparing <sup>13</sup>C<sub>2</sub>F<sub>4</sub> as the compound needed to obtain the desired isotropic spectrum of the <sup>13</sup>C-labeled *c*-C<sub>4</sub>F<sub>8</sub><sup>•-</sup>. (See Supporting Information for additional experimental details.)

### 3. Computational Methods

Two double- $\zeta$  basis sets (denoted 6-31+G(*d*) and DZP+) and two triple- $\zeta$  basis sets (denoted 6-311+G(2*df*) and TZ2P(*f*+) were employed in this study. (MP2 calculations with the triple- $\zeta$  basis sets (6-311+G(2*df*) and TZ2P(*f*+) were not feasible for the decafluorocyclopentane species.) Full geometry optimizations were carried out with the B3LYP density functional<sup>43,44</sup> and the MP2 method.<sup>45</sup> Harmonic

vibrational frequencies were computed with the B3LYP functional and, whenever possible, at the MP2 level of theory to confirm that optimized structures were minima on the potential energy surface and to obtain zero-point vibrational energy corrections to the electronic energies. See Supporting Information for additional computational details.

Adiabatic electron affinities (AEA) were calculated at all of the aforementioned levels of theory and determined as the difference between the electronic energy of the optimized neutral structure and that of the optimized anion structure. The hyperfine coupling constants (hfcc's) were computed at both the B3LYP and MP2 levels of theory. Two different types of MP2 calculations were performed. The MP2 hfcc's were computed not only with the frozen core/deleted virtual approximations described in the Supporting Information but also with all electrons correlated and all orbitals active (denoted MP2(FC) and MP2(ALL), respectively).

### 4. ESR Results

**Hexafluorocyclopropane Radical Anion.** As shown in Figure 1, the isotropic ESR spectrum of *c*-C<sub>3</sub>F<sub>6</sub><sup>•-</sup> generated by electron attachment to *c*-C<sub>3</sub>F<sub>6</sub> in the HME matrix is remarkably clean and well resolved. All of the second-order (*M*<sub>1</sub>, *I*) components expected from hyperfine interaction with six equivalent fluorines (*I*(<sup>19</sup>F) = 1/2) are clearly displayed except for the two innermost *M*<sub>1</sub> = 0 (*I* = 1, 0) lines which are obscured by the intense signals from the HME matrix radicals<sup>46</sup> in the congested central region. Due to the large *a*(<sup>19</sup>F) coupling constant of 198.6 G (Table 1), the predicted second-order splittings in the 1:6:15:20:15:6:1 first-order binomial pattern (see stick diagram in Figure 1 for the second-order hyperfine structure) are appreciable, these being 36.3 G ( $3a^2/H$ ) for the *M*<sub>1</sub> =  $\pm 2$  (*I* = 3, 2) line groups and 36.3 G ( $3a^2/H$ ) and 24.2 G ( $2a^2/H$ ) for the *M*<sub>1</sub> =  $\pm 1$  (*I* = 3, 2, 1) line groups. The measured splittings are within  $\pm 0.5$  G of these expectations, confirming the spectral analysis in terms of the identical coupling of 198.6 G to six <sup>19</sup>F nuclei.

Given the strong signals of the spectral lines in Figure 1, it is remarkable that there is no indication of a weak satellite spectrum in natural abundance resulting from an additional interaction with a single <sup>13</sup>C nucleus. Although the total intensity of this <sup>13</sup>C satellite pattern is expected to be only ca. 3% of that for the main spectrum, the corresponding <sup>13</sup>C satellite spectra consisting of superimposed doublet patterns have been observed for both C<sub>6</sub>F<sub>6</sub><sup>•-</sup> and C<sub>2</sub>F<sub>4</sub><sup>•-</sup> in natural abundance.<sup>37,40</sup> In these latter cases, however, the <sup>13</sup>C doublet splitting is large enough (12.1 and 48.7 G, respectively) so that the weak satellite lines are sufficiently displaced from the main spectrum to be resolved. On the other hand, should the <sup>13</sup>C coupling be comparable to or less than the line width (5–10 G), the flanking satellite features would be buried inside the much stronger lines of the main spectrum and therefore unobservable. By analogy, this latter interpretation of the “missing” satellite lines gains credence from the fact that <sup>13</sup>C satellite signals are also not observed in the intense spectrum of the naturally abundant *c*-C<sub>4</sub>F<sub>8</sub><sup>•-</sup>, a result that is clearly attributable to the finding of only a small <sup>13</sup>C coupling of 5.2 G in the <sup>13</sup>C-enriched *c*-C<sub>4</sub>F<sub>8</sub><sup>•-</sup> (vide infra). We conclude therefore that the upper limit for the <sup>13</sup>C coupling in *c*-C<sub>3</sub>F<sub>6</sub><sup>•-</sup> is not more than 10 G.

**Octafluorocyclobutane Radical Anion.** As mentioned in the Experimental Methods, it was possible to generate *c*-C<sub>4</sub>F<sub>8</sub><sup>•-</sup> in HME from both *c*-C<sub>4</sub>F<sub>8</sub> and C<sub>2</sub>F<sub>4</sub>. The well-resolved ESR

(38) Adam, W.; Walter, H.; Chen, G.-F.; Williams, F. *J. Am. Chem. Soc.* **1992**, *114*, 3007.

(39) Nelsen, S. F.; Reinhart, L. A.; Tran, H. A.; Clark, T.; Chen, G.-F.; Pappas, R. S.; Williams, F. *Chem.—Eur. J.* **2002**, *8*, 1074.

(40) McNeil, R. I.; Shiotani, M.; Williams, F.; Yim, M. B. *Chem. Phys. Lett.* **1977**, *51*, 433.

(41) McNeil, R. I.; Shiotani, M.; Williams, F.; Yim, M. B. *Chem. Phys. Lett.* **1977**, *51*, 438.

(42) The anisotropic spectrum of *c*-C<sub>4</sub>F<sub>8</sub><sup>•-</sup> in MTHF is a complicated powder pattern<sup>41</sup> quite unsuitable for the determination of the principal values of the <sup>13</sup>C hyperfine tensor in a <sup>13</sup>C-enriched sample.

(43) Lee, C.; Yang, W.; Parr, R. G. *Phys. Rev. B* **1988**, *37*, 785.

(44) Becke, A. D. *J. Chem. Phys.* **1993**, *98*, 5648–5652.

(45) Møller, C.; Plesset, M. *Phys. Rev.* **1934**, *46*, 618.

(46) Wang, J. T.; Williams, F. *Chem. Phys. Lett.* **1979**, *67*, 202.

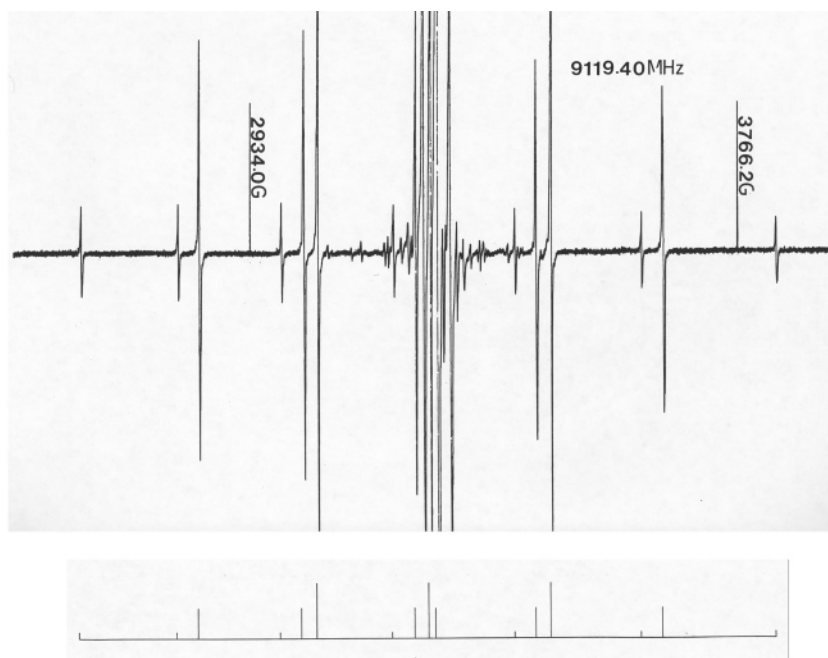


**Figure 1.** ESR spectrum of a solid solution of 1 mol % of hexafluorocyclopropane in the hexamethylethane matrix after  $\gamma$ -irradiation at 77 K (dose, 0.5 Mrad) and subsequent warming to 160 K. Apart from the additional central lines resulting from a mixture of alkyl radicals derived from the matrix (see ref 46), the spectrum consists almost entirely of the components expected for a radical with six equivalent  $I = 1/2$  nuclei and a large hyperfine coupling constant (198.6 G), as represented by the stick diagram. It can be seen that the high-resolution spectrum displays the full second-order structure for such a radical, and it is therefore assigned to the negative ion of hexafluorocyclopropane ( $c\text{-C}_3\text{F}_6^{\cdot-}$ ).

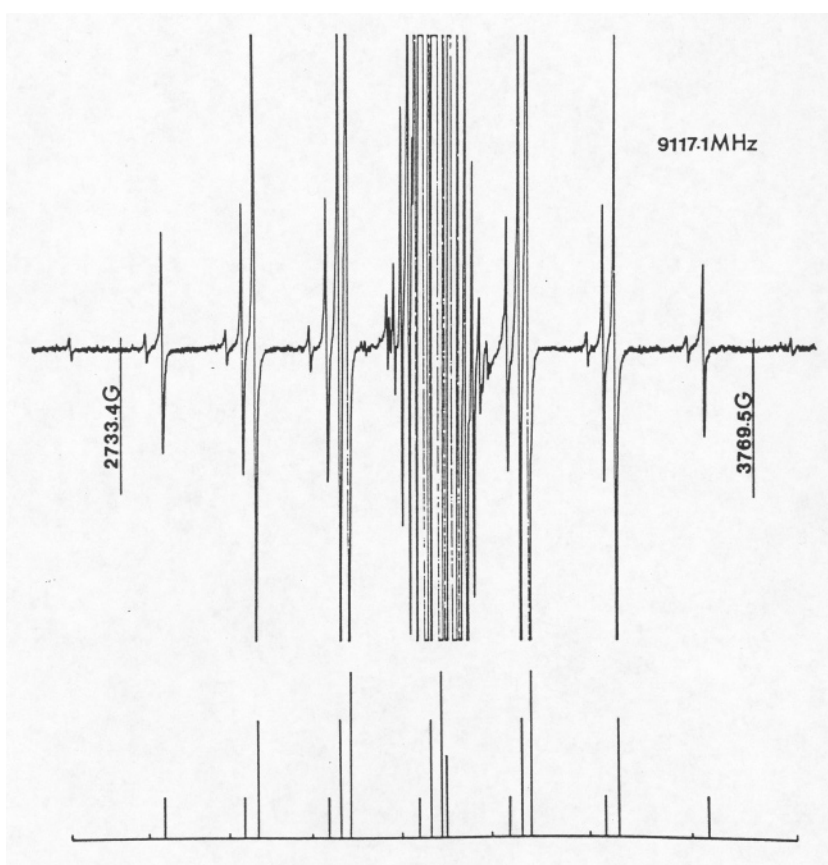


**Figure 2.** ESR spectrum of a solid solution of 1 mol % of octafluorocyclobutane in the hexamethylethane matrix after  $\gamma$ -irradiation at 77 K (dose, 0.5 Mrad) and subsequent warming to 163 K. As in Figure 1, the congested central region includes lines from matrix radicals, but otherwise the spectrum is dominated by the line components expected for a radical with eight equivalent  $I = 1/2$  nuclei and a large hyperfine coupling constant (147.6 G), as represented by the stick diagram. The spectrum is therefore assigned to the negative ion of octafluorocyclobutane ( $c\text{-C}_4\text{F}_8^{\cdot-}$ ).

spectrum derived from  $c\text{-C}_4\text{F}_8$  is shown in Figure 2 and is immediately recognizable from the accompanying stick diagram

as a second-order isotropic hyperfine pattern resulting from the presence of eight equivalent spin- $1/2$  nuclei in the signal carrier.

**Table 1.** Experimental  $^{19}\text{F}$  and  $^{13}\text{C}$  Isotropic Hyperfine Coupling Constants and  $g$ -factors for the Perfluorocycloalkane Negative Ions,  $c\text{-C}_n\text{F}_{2n}^{\bullet-}$  ( $n = 3\text{--}5$ ), from Matrix ESR Studies

	$a(^{19}\text{F})/\text{G}$		$a(^{13}\text{C})/\text{G}$		$g$
$c\text{-C}_3\text{F}_6^{\bullet-}$	$198.6 \pm 0.4$	(6F)	$<10^a$	(1 $^{13}\text{C}$ )	$2.0027 \pm 0.0006$
$c\text{-C}_4\text{F}_8^{\bullet-}$	$147.6 \pm 0.4^b$	(8F)	$5.2 \pm 0.4$	(4 $^{13}\text{C}$ )	$2.0021 \pm 0.0008$
$c\text{-C}_5\text{F}_{10}^{\bullet-}$	$117.9 \pm 0.4$	(10F)	$<10^a$	(1 $^{13}\text{C}$ )	$2.0027 \pm 0.0006$

<sup>a</sup> See text for a fuller discussion of this estimate to the upper limit; essentially, the weak signals expected from a superimposed  $^{13}\text{C}$  doublet pattern in natural abundance were not resolved within the line widths of the main  $^{12}\text{C}$  spectrum. <sup>b</sup> An approximate value of 151 G for the  $^{19}\text{F}$  hyperfine coupling in  $c\text{-C}_4\text{F}_8^{\bullet-}$  has been derived independently from studies of the magnetic-field effect on the recombination fluorescence of the anthracene radical cation with  $c\text{-C}_4\text{F}_8^{\bullet-}$  in isooctane solution at 296 K (Grigoryants, V. M.; McGrane, S. D.; Lipsky, S. J. *Chem. Phys.* **1998**, *109*, 7354). The magnetic-field positions observed for the level-crossing resonances are predicted by the theory of a hyperfine-driven spin evolution on the  $c\text{-C}_4\text{F}_8^{\bullet-}$ . The modulation amplitude of 25 G used in these experiments resulted in broad resonance lines, and therefore the  $^{19}\text{F}$  hfc obtained in this way is expected to be less accurate than the ESR value.

The coupling constant  $a(^{19}\text{F})$  of  $147.6 \pm 0.4$  G was determined from the higher-order line positions. Additionally, in the order from low to high field, the measured second-order splittings of 26.6 G, 26.6\_20.0 G, and 26.6\_20.0\_13.3 G in the  $M_I = \pm 3$ ,  $\pm 2$ , and  $\pm 1$  groups are in excellent agreement with the predicted values of  $4a^2/H$ ,  $4a^2/H\text{-}3a^2/H$ , and  $4a^2/H\text{-}3a^2/H\text{-}2a^2/H$ , respectively, and there can be little doubt about the assignment to  $c\text{-C}_4\text{F}_8^{\bullet-}$ . As noted in discussing the  $c\text{-C}_3\text{F}_6^{\bullet-}$  spectrum, there is no indication of a weak  $^{13}\text{C}$  satellite spectrum despite the strong line intensities.

Turning to the spectrum generated from  $\text{C}_2\text{F}_4$  in HME and shown in Figure 3, it is clear that the strongest pattern is identical to that just described for  $c\text{-C}_4\text{F}_8^{\bullet-}$ . However, examination of the spectral region lying within the  $M_I = \pm 2$  groups of the  $c\text{-C}_4\text{F}_8^{\bullet-}$  spectrum reveals a much weaker set of lines corresponding to the  $M_I = \pm 2$  and  $\pm 1$  components of  $\text{C}_2\text{F}_4$  with a coupling constant  $a(^{19}\text{F})$  of 96.2 G, consistent with the previous determination<sup>40</sup> of 94.3 G from the spectrum of  $\text{C}_2\text{F}_4$  in the tetramethylsilane matrix.<sup>47</sup> Thus, it can be inferred that most of the  $\text{C}_2\text{F}_4$  formed initially by electron attachment is converted in the HME matrix to  $c\text{-C}_4\text{F}_8^{\bullet-}$  as a result of the known bimolecular reaction with  $\text{C}_2\text{F}_4$ .<sup>41</sup> The importance of this finding is that it allows the  $^{13}\text{C}$ -labeled  $\text{C}_2\text{F}_4$  to be used as the precursor to generate the isotropic spectrum of  $c\text{-}^{13}\text{C}_4\text{F}_8^{\bullet-}$  and thereby obtain the  $^{13}\text{C}$  coupling constant, as discussed below.

**$^{13}\text{C}$ -labeled Octafluorocyclobutane Radical Anion.** The  $^{13}\text{C}$ -labeled  $\text{C}_2\text{F}_4$  precursor was prepared by the IR laser photolysis of  $^{13}\text{CHClF}_2$  that in turn was prepared from  $^{13}\text{CHCl}_3$ , as described in the Supporting Information. In consequence, this  $^{13}\text{C}_2\text{F}_4$  product inevitably contained various other halogen compounds as impurities. On irradiation, such compounds can compete very effectively with the  $^{13}\text{C}_2\text{F}_4$  for the electrons with the result that the ESR signal intensity from the generated  $c\text{-}^{13}\text{C}_4\text{F}_8$  was found to be much lower than that observed in the experiments described with the high purity  $\text{C}_2\text{F}_4$ . Fortunately, this loss of absolute signal intensity in the desired  $c\text{-}^{13}\text{C}_4\text{F}_8^{\bullet-}$  spectrum was not accompanied by strong masking signals from the other products of electron capture. This spectral selectivity undoubtedly results from the fact that the  $c\text{-C}_4\text{F}_8^{\bullet-}$  spectrum in

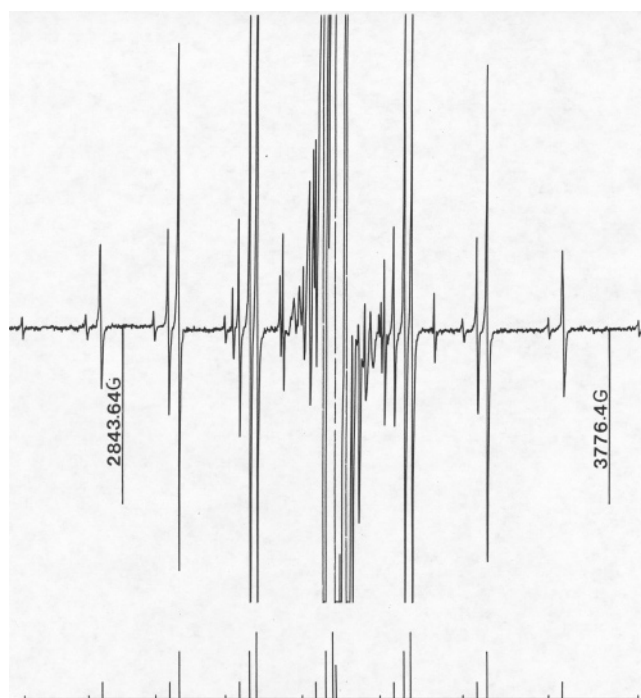


**Figure 3.** ESR spectrum of a solid solution of 4 mol % of tetrafluoroethylene in the hexamethylethane matrix after  $\gamma$ -irradiation at 77 K (dose, 0.5 Mrad) and subsequent warming to 174 K. By comparison with Figure 2, the main spectrum represented by the stick diagram is clearly that of the negative ion of octafluorocyclobutane ( $c\text{-C}_4\text{F}_8^{\bullet-}$ ) resulting from the addition of  $\text{C}_2\text{F}_4^{\bullet-}$  to  $\text{C}_2\text{F}_4$  (see ref 41) in this soft matrix. The additional weaker lines contained within the  $M_I = \pm 2$  components of the  $c\text{-C}_4\text{F}_8^{\bullet-}$  spectrum are due to the spectrum of  $\text{C}_2\text{F}_4^{\bullet-}$  (see ref 40) with a hyperfine coupling constant of 96.2 G. The  $M_I = \pm 2$  and  $\pm 1$  components of the latter spectrum are clearly displayed since they are not overlapped by the lines from the more intense  $c\text{-C}_4\text{F}_8^{\bullet-}$  spectrum.

HME is isotropic with narrow lines, whereas the matrix ESR spectra of many halogen-containing radicals and radical ions consist of broad anisotropic patterns characterized by very low signal intensities.

In view of the weak  $c\text{-}^{13}\text{C}_4\text{F}_8^{\bullet-}$  signals from the  $\gamma$ -irradiated  $^{13}\text{C}_2\text{F}_4$  sample, a direct comparison was sought with the  $c\text{-}^{12}\text{C}_4\text{F}_8^{\bullet-}$  spectrum generated from the reference  $^{12}\text{C}_2\text{F}_4$  sample similarly prepared by IR laser photolysis. In this way, with similar overall signal intensities, it was expected that the additional  $^{13}\text{C}$  hyperfine structure in the  $c\text{-}^{13}\text{C}_4\text{F}_8^{\bullet-}$  spectrum would be more clearly delineated against that of a  $c\text{-}^{12}\text{C}_4\text{F}_8^{\bullet-}$  background, and Figure 4 presents such a comparison of the  $M_I(^{19}\text{F}) = \pm 2$  line groups taken from the spectra of  $c\text{-}^{12}\text{C}_4\text{F}_8^{\bullet-}$  (top set) and  $c\text{-}^{13}\text{C}_4\text{F}_8^{\bullet-}$  (bottom set). First, it should be noted that the weakest low-field  $I(^{19}\text{F}) = 4$  component is detectable at only just above the noise level, as revealed most clearly in the  $M_I(^{19}\text{F}) = +2$  group of the  $c\text{-}^{12}\text{C}_4\text{F}_8^{\bullet-}$  spectrum (top left). Therefore, the analysis is necessarily restricted to the  $I(^{19}\text{F}) = 3$  and 2 components which are seen to be present in the  $c\text{-}^{12}\text{C}_4\text{F}_8^{\bullet-}$  spectrum with the expected intensity ratios 7 and 20 relative to that of the weakest  $I(^{19}\text{F}) = 4$  component. Most significantly, at the low- and high-field positions of these single lines in the  $c\text{-}^{12}\text{C}_4\text{F}_8^{\bullet-}$  spectrum (top set), the corresponding resonances in the  $c\text{-}^{13}\text{C}_4\text{F}_8^{\bullet-}$  spectrum (bottom set) consist of closely spaced 1:4:6:4:1 hyperfine patterns, as expected for coupling to four equivalent  $^{13}\text{C}$  nuclei. Measurements of these splittings (see the overlapping stick-diagram reconstructions in

(47) On close examination, the line shapes of the  $\text{C}_2\text{F}_4^{\bullet-}$  spectrum in tetramethylsilane<sup>40</sup> (TMS) show a slight anisotropy, which could account for the difference of 1.9 G in the  $a(^{19}\text{F})$  values of the spectra obtained in the TMS and HME matrices.

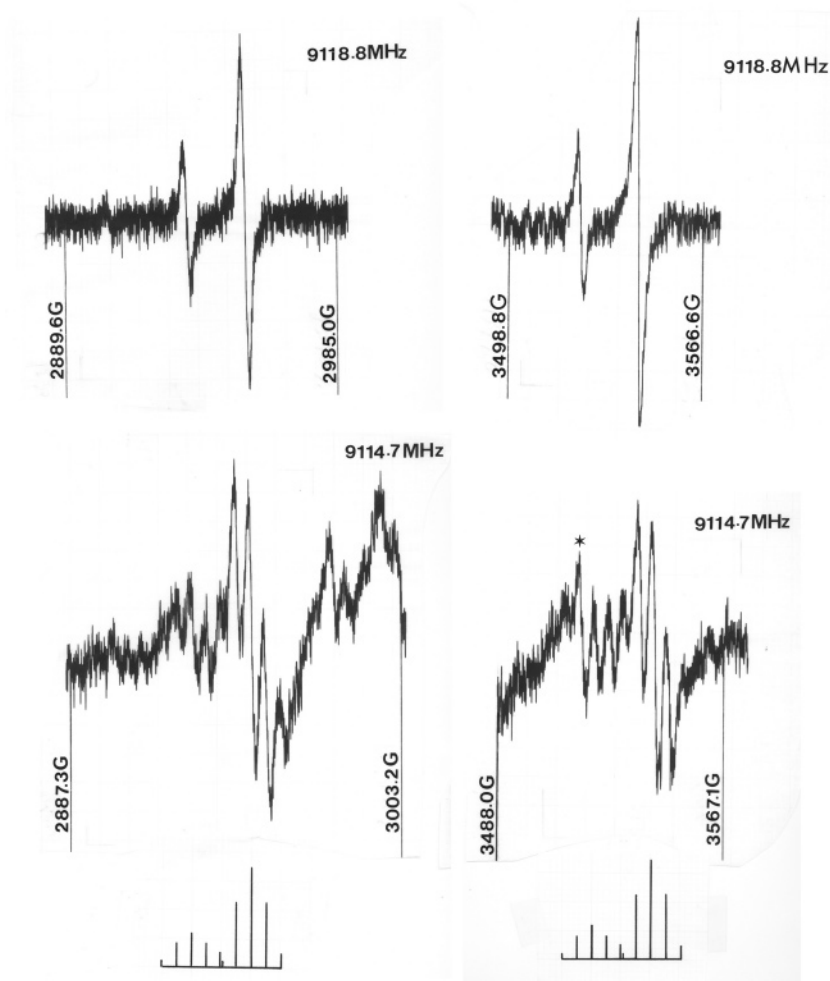


**Figure 4.** Comparison of the  $M_I(^{19}\text{F}) = \pm 2$  sets of hyperfine components taken from the ESR spectra of  $c\text{-}^{12}\text{C}_4\text{F}_8^{\bullet-}$  (upper spectra) and  $c\text{-}^{13}\text{C}_4\text{F}_8^{\bullet-}$  (lower spectra) showing the additional lines in the lower spectra resulting from splitting by the four equivalent  $^{13}\text{C}$  nuclei ( $I = 1/2$ ). These are represented by the 1:4:6:4:1 binomial quintet structures shown in the stick diagrams for the  $I(^{19}\text{F}) = 3$  and 2 spectral components. The spectra were generated from  $\text{C}_2\text{F}_4$  and  $^{13}\text{C}_2\text{F}_4$  as described in Figure 3, and the  $^{13}\text{C}$  hyperfine splitting constant of the negative ion of octafluorocyclobutane is thereby shown to be 5.2 G (see text).

Figure 4) reveal that the  $^{13}\text{C}$  coupling constant in  $c\text{-}^{13}\text{C}_4\text{F}_8^{\bullet-}$  is  $5.2 \pm 0.4$  G.

**Decafluorocyclopentane Radical Anion.** In the ESR spectra of  $c\text{-C}_5\text{F}_{10}^{\bullet-}$  shown in Figure 5, the pattern again corresponds to the equivalence of all the fluorines. Indeed, all 10  $M_I$  line groups ( $\pm 5, \pm 4, \pm 3, \pm 2, \pm 1$ ) that are outside the congested center ( $M_I = 0$ ) region are of textbook clarity with sufficient signal-to-noise ratios that the two outermost lines ( $M_I = \pm 5$ , each with strength 1 out of the total  $2^{10} = 1024$  spectral intensity) can be seen in the wings of the upper spectrum. The measured second-order splittings of 21.4, 17.1, 12.8, and 8.6 G in the  $M_I = \pm 4, \pm 3, \pm 2, \pm 1$  line groups are in excellent accord with the predicted values given by the 5, 4, 3, and 2 multiples of  $a^2/H$  (4.28 G) based on the value of  $a(^{19}\text{F})$  of  $117.9 \pm 0.4$  G determined from the fit to the higher-order line positions.

## 5. Computational Results

**$c\text{-C}_3\text{F}_6$  and  $c\text{-C}_3\text{F}_6^{\bullet-}$ .** Both hexafluorocyclopropane and its negative ion have a  $D_{3h}$  geometry (see Figure 6). The Cartesian coordinates of all optimized structures can be found in the Supporting Information. A significant geometrical distortion occurs as the electron is added to  $c\text{-C}_3\text{F}_6$  to form  $c\text{-C}_3\text{F}_6^{\bullet-}$ ; the C–C bond lengths contract by at least 0.08 Å, and the C–F

bond lengths increase by at least 0.10 Å. This trend is consistently predicted at each level of theory since the optimized geometrical parameters exhibit very little dependence on method and basis set. (As different methods and basis sets are used, the bond lengths change by no more than 0.028 Å, and bond angles, by no more than 0.24°.) The electronic ground state of  $c\text{-C}_3\text{F}_6^{\bullet-}$  is  $^2A_2''$  at all levels of theory. Table 2 lists  $^{13}\text{C}$  and  $^{19}\text{F}$  hyperfine coupling constants of  $c\text{-C}_n\text{F}_{2n}^{\bullet-}$  ( $n = 3\text{--}5$ ). Errors relative to the experimental  $^{19}\text{F}$  hfcc's of  $c\text{-C}_3\text{F}_6^{\bullet-}$  in Table 1 range from 6% to 10% for the B3LYP functional and 1–8% for the MP2 method. The vast majority of the spin density lies on the three equivalent C atoms. Mulliken spin densities range from 0.25 to 0.28 for the spin unrestricted B3LYP calculations and 0.28–0.32 for the MP2 calculations with a spin unrestricted Hartree–Fock (UHF) reference. Figure 7a shows the nodal structure along the C–F bonds associated with the  $5a_2''$  singly occupied molecular orbital (SOMO) which is consistent with the geometrical distortions (vide supra).

**$c\text{-C}_4\text{F}_8$  and  $c\text{-C}_4\text{F}_8^{\bullet-}$ .** The  $c\text{-C}_4\text{F}_8^{\bullet-}$  species adopts a  $D_{4h}$  geometry as its equilibrium structure, while the neutral counterpart has a puckered  $D_{2d}$  geometry as shown in Figure 6. Again, the C–C bond lengths decrease, and the C–F bond lengths increase on electron capture (both by at least 0.06 Å).

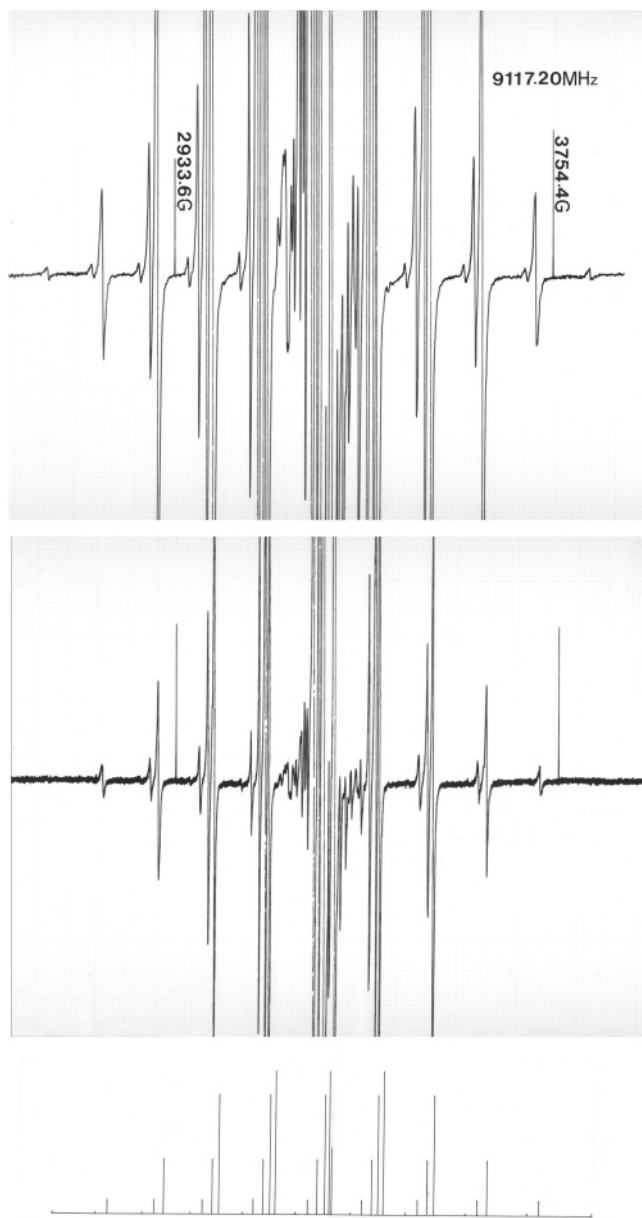


**Figure 5.** ESR spectra of a solid solution of 1 mol % of decafluorocyclopentane in the hexamethylethane matrix after  $\gamma$ -irradiation at 77 K (dose, 0.5 Mrad) and subsequent warming to 165 K recorded under different instrumental conditions. As in Figures 1, 2, and 3, the congested central regions include lines from matrix radicals but otherwise the spectra are dominated by the line components expected for a radical with 10 equivalent  $I = 1/2$  nuclei and a large hyperfine coupling constant (117.9 G), as represented by the stick diagram. The signal-to-noise ratio in the upper spectrum is sufficient to reveal the weakest outermost  $M_I(^{19}\text{F}) = \pm 5$  lines in the wings. The spectrum is therefore assigned to the negative ion of decafluorocyclopentane ( $c\text{-C}_5\text{F}_{10}^{\bullet-}$ ).

The optimized geometrical parameters continue to exhibit little variation between method and basis set. The extent of the ring puckering is the only exception where the CCCC torsional angle is approximately  $16^\circ$  at the MP2 level but closer to  $8^\circ$  with the B3LYP density functional. All calculations indicate that the ground state of  $c\text{-C}_4\text{F}_8^{\bullet-}$  is  $^2\text{A}_{2u}$ . Computed  $^{19}\text{F}$  hfcc's in Table 2 deviate by 3–9% at the B3LYP level of theory from the experimental values in Table 1. MP2 values deviate by 1–5%. As with  $c\text{-C}_3\text{F}_6^{\bullet-}$ , the spin density of the unpaired electron resides almost exclusively on the equivalent C atoms. Spin

unrestricted B3LYP calculations indicate the Mulliken spin density is 0.20–0.24 on each C atom, while that of the analogous MP2 data is 0.22–0.27. The SOMO ( $5a_{2u}$ ) is plotted in Figure 7b, once again illustrating the node along the C–F bonds.

**$c\text{-C}_5\text{F}_{10}$  and  $c\text{-C}_5\text{F}_{10}^{\bullet-}$ .** Unlike the other two cyclic anions examined in the current study, the carbon atoms are not coplanar in the minimum energy structure of  $c\text{-C}_5\text{F}_{10}^{\bullet-}$  which belongs to the  $C_s$  point group (Figure 6). All levels of theory confirm that the electronic ground state of this structure is  $^2\text{A}'$ . For the neutral counterpart, the nature of the B3LYP potential energy surface (PES) exhibits a dependence on the class of basis set used. The split valence basis sets [6-31+G( $d$ ) and 6-311+G-2( $df$ )] indicate that the  $C_s$  structure of  $c\text{-C}_5\text{F}_{10}$  is a minimum on the PES, while the Huzinaga–Dunning basis sets (DZP+ and TZ2P( $f$ )+) indicate that it is a transition state. Using larger numerical integration grids does not resolve this discrepancy. Since MP2 analytic frequency computations were not feasible for  $c\text{-C}_5\text{F}_{10}$ , a series of RHF optimizations and frequency computations were carried out. All RHF calculation, regardless of basis set, indicate that the  $C_s$  structure is a transition state. A  $C_1$  minimum was located that deviates only slightly from  $C_s$  symmetry and lies no more than 0.02 kcal/mol below the  $C_s$  transition state. Since this minute energy difference has no effect on the electron affinities reported in Table 3, the MP2 optimizations of  $c\text{-C}_5\text{F}_{10}$  were carried out in  $C_s$  symmetry.

The fact that all five carbon atoms are not chemically equivalent in the optimized structure of the decafluorocyclopentane anion at first appears to be inconsistent with the experimental ESR spectrum. A rigid  $C_s$  structure with five symmetry unique C atoms should produce six  $^{19}\text{F}$  hfcc's (separated by as many as 111 G at the MP2/6-31+G( $d$ ) level of theory), but only one hfcc is observed in the ESR spectrum. This discrepancy can be reconciled since the high symmetry  $D_{5h}$  structure (a degenerate second-order saddle point) lies less than 0.2 kcal/mol above the minimum energy  $C_s$  structure at all levels of theory. This minute electronic energy difference indicates the mechanism that renders the five  $>\text{CF}_2$  groups equivalent readily occurs even at the low temperatures of the matrix (ca. 160–170 K). At these temperatures, it is likely that this inversion process occurs on a time scale that is much faster than that associated with small  $^{19}\text{F}$  hfcc differences present in the  $C_s$  structure. Under such conditions, an identical  $^{19}\text{F}$  hyperfine coupling to all 10 fluorines (corresponding to the average environment of the F atoms) will be observed.

Indeed, the average hyperfine coupling values obtained for the  $C_s$  structure are in excellent agreement with the experimental data. The calculations indicate an average  $a(^{19}\text{F})$  value that ranges from 108.2 to 115.5 G (a 2–8% deviation from experiment) at the B3LYP level of theory and 119.1–122.0 G (a 1–4% deviation from experiment) at the MP2 level of theory. It should be noted, however, that this impressive accuracy of the computed hfcc's may not extend to other systems. In addition, the C atoms have nearly identical spin densities even though they are not equivalent. For any particular method and basis set, the spin densities of nonequivalent C atoms vary by less than 0.02. As observed with  $c\text{-C}_3\text{F}_6^{\bullet-}$  and  $c\text{-C}_4\text{F}_8^{\bullet-}$ , essentially all of the spin density of the unpaired electron resides on the C atoms (0.17–0.20 at the B3LYP level and 0.18–0.23 at the MP2 level).

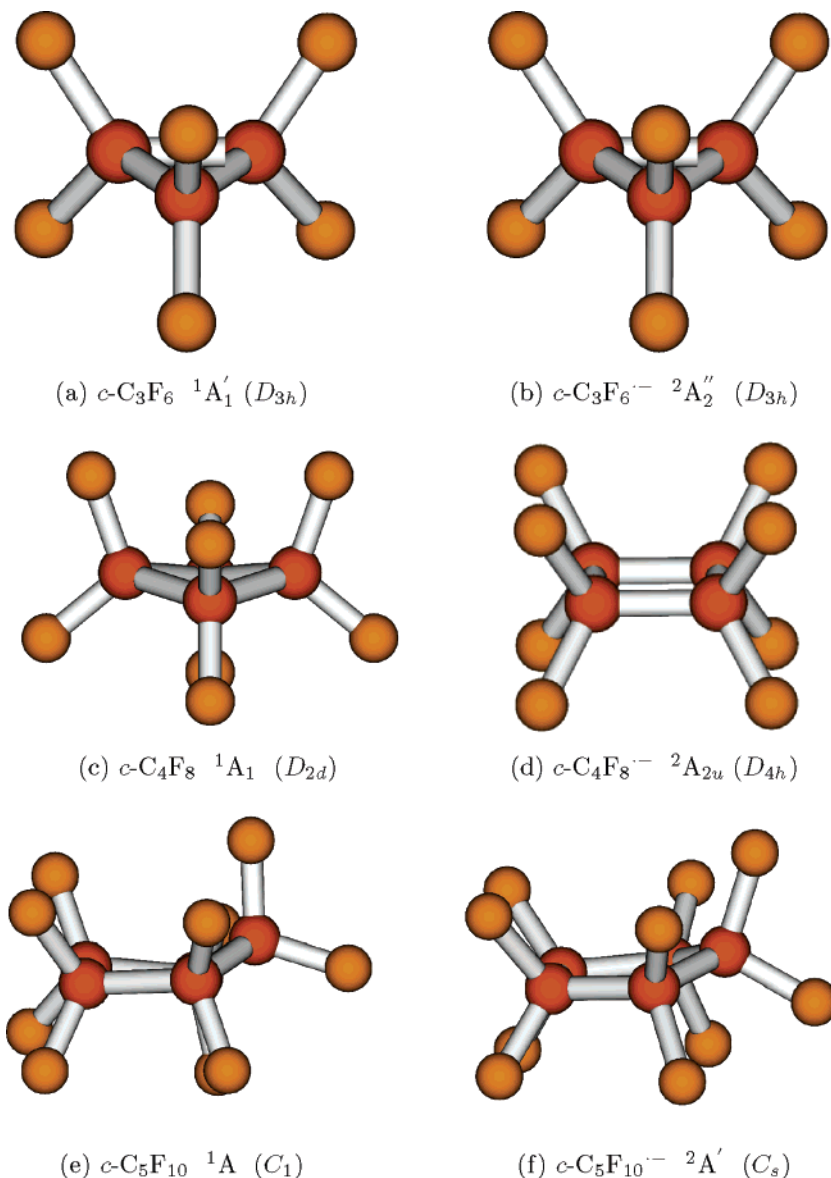


**Figure 6.** Equilibrium structures, ground electronic states, and point group symmetries (in parentheses) of the perfluorocycloalkanes and their negative ions.

**Table 2.**  $c\text{-C}_3\text{F}_6^-$ ,  $c\text{-C}_4\text{F}_8^-$ , and  $c\text{-C}_5\text{F}_{10}^-$  Computed Hyperfine Coupling Constants in Gauss (G). MP2(FC) and MP2(ALL) Denote Frozen Core and All Electron MP2 Calculations, Respectively

method	basis	$c\text{-C}_3\text{F}_6^-$		$c\text{-C}_4\text{F}_8^-$		$c\text{-C}_5\text{F}_{10}^{-a}$	
		$a(^{13}\text{C})/\text{G}$	$a(^{19}\text{F})/\text{G}$	$a(^{13}\text{C})/\text{G}$	$a(^{19}\text{F})/\text{G}$	$a(^{13}\text{C})/\text{G}$	$a(^{19}\text{F})/\text{G}$
B3LYP	6-31+G( <i>d</i> )	+4.6	+178.8	+2.2	+138.2	+1.2	+114.1
	DZP+	-3.7	+186.6	-4.6	+142.5	-4.5	+115.5
	6-311+G(2 <i>df</i> )	-5.3	+177.9	-5.4	+134.1	-5.1	+108.2
	TZ2P( <i>f</i> )+	-5.0	+184.5	-5.2	+139.5	-4.8	+112.5
MP2(ALL)	6-31+G( <i>d</i> )	+9.9	+182.6	+4.8	+140.5	+2.6	+119.3
	DZP+	+0.2	+201.5	-3.6	+152.0	-4.7	+122.2
	6-311+G(2 <i>df</i> )	-2.0	+191.8	-4.1	+141.0		
	TZ2P( <i>f</i> )+	-1.8	+197.9	-4.0	+148.2		
MP2(FC)	6-31+G( <i>d</i> )	+10.0	+182.1	+4.9	+140.1	+2.7	+119.1
	DZP+	+0.2	+200.9	-3.6	+151.6	-4.7	+122.0
	6-311+G(2 <i>df</i> )	-2.0	+190.1	-4.1	+139.7		
	TZ2P( <i>f</i> )+	-1.8	+196.8	-4.0	+147.3		
EXPT		<10	198.6 ± 0.4	5.2 ± 0.4	147.6 ± 0.4	<10	117.9 ± 0.4

<sup>a</sup> Average values from the  $C_s$  structure with three chemically unique C atoms and six chemically unique F atoms.

<sup>13</sup>C hfcc's. The exceptional quantitative agreement between the theoretical and experimental <sup>19</sup>F hfcc's does not extend to the <sup>13</sup>C hfcc's. Recall that the  $a(^{19}\text{F})$  values computed at the

MP2 level with the TZ2P(*f*)+ basis set (Table 2) deviate by less than 1% from the experimental data reported in Table 1, regardless of whether the core electrons were correlated in the

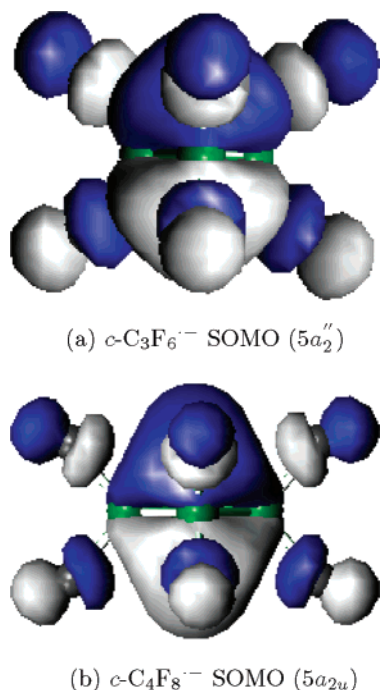


**Figure 7.** Plots of the singly occupied molecular orbitals (SOMO) of  $c\text{-C}_3\text{F}_6^{\bullet-}$  and  $c\text{-C}_4\text{F}_8^{\bullet-}$ .

**Table 3.**  $c\text{-C}_3\text{F}_6^{\bullet-}$ ,  $c\text{-C}_4\text{F}_8^{\bullet-}$ , and  $c\text{-C}_5\text{F}_{10}^{\bullet-}$  Adiabatic Electron Affinities (AEA) and Zero-Point Vibrational Energy Corrections ( $\delta\text{ZPVE}$ ) at Various Levels of Theory; All Values Are in eV

method	basis	$c\text{-C}_3\text{F}_6^{\bullet-}$		$c\text{-C}_4\text{F}_8^{\bullet-}$		$c\text{-C}_5\text{F}_{10}^{\bullet-}$	
		AEA	$\delta\text{ZPVE}$	AEA	$\delta\text{ZPVE}$	AEA	$\delta\text{ZPVE}$
B3LYP	6-31+G( <i>d</i> )	+0.57	+0.17	+0.95	+0.18	+1.00	+0.18
	DZP+	+0.47	+0.17	+0.86	+0.18	+0.94	+0.18
	6-311+G(2 <i>df</i> )	+0.42	+0.17	+0.80	+0.18	+0.87	+0.17
	TZ2P( <i>f</i> )+	+0.40	+0.17	+0.80	+0.17	+0.86	+0.17
MP2	6-31+G( <i>d</i> )	+0.26	+0.15	+0.64	+0.18	+0.63 <sup>a</sup>	
	DZP+	+0.11	+0.16	+0.51	+0.17	+0.51 <sup>a</sup>	
	6-311+G(2 <i>df</i> )	+0.02		+0.43			
	TZ2P( <i>f</i> )+	+0.10		+0.52			

<sup>a</sup> Computed using a  $C_s$  structure as the reference for the neutral species. See text for a fuller explanation.

MP2 calculations. For the  $^{13}\text{C}$  hfcc's, however, comparison of the experimental and theoretical data is more complicated. In all cases, the magnitude of the calculated  $^{13}\text{C}$  hfcc's is small which is in qualitative agreement with the experiment. Since only an upper bound (10 G) could be established for  $c\text{-C}_3\text{F}_6^{\bullet-}$  and  $c\text{-C}_5\text{F}_{10}^{\bullet-}$ , there is only one reliable data point for comparison. A detailed discussion of the  $a(^{13}\text{C})$  values for  $c\text{-C}_4\text{F}_8^{\bullet-}$  is presented in Section 6.

**Electron Affinities.** The adiabatic electron affinities (AEAs) of all three neutral species are collected in Table 3 along with the zero-point vibrational energy corrections to the AEAs ( $\delta\text{ZPVE}$ ). Zero-point corrections are remarkably consistent and increase the AEA by  $\sim 0.17$  eV regardless of the molecule, method, or basis set. The AEAs of  $c\text{-C}_4\text{F}_8$  and  $c\text{-C}_5\text{F}_{10}$  are very similar and roughly twice that of  $c\text{-C}_3\text{F}_6$ . With the B3LYP density functional, the AEAs for  $c\text{-C}_4\text{F}_8$  and  $c\text{-C}_5\text{F}_{10}$  lie near 0.9 eV, while that of  $c\text{-C}_3\text{F}_6$  falls near 0.5 eV. When the MP2 method is used, these values decrease to 0.5 and 0.1 eV, respectively. Extensive calibration has shown that AEAs computed with the B3LYP functional and the DZP+ basis set tend to lie within 0.3 eV of the experimental values for electron

affinities involving an open-shell anion and closed-shell neutral molecule.<sup>48</sup> In fact, this model chemistry has been used to determine the electron affinities of several families of closely related perfluorinated compounds.<sup>49–53</sup> These recent studies have pointed out the limited availability of experimental data for these important species, an issue the present investigation is helping address.

## 6. Discussion

Since the most detailed ESR results have been obtained for  $c\text{-C}_4\text{F}_8^{\bullet-}$  we will examine this anion in greater detail. All the theoretical methods used in this investigation predict that  $c\text{-C}_4\text{F}_8^{\bullet-}$  adopts a  $D_{4h}$  geometry with a  ${}^2A_{2u}$  ground state, and the calculations of the isotropic  $^{19}\text{F}$  and  $^{13}\text{C}$  hyperfine coupling constants for this state (Table 2) will now be compared with the ESR results given in Table 1. First, the experimental  $a(^{19}\text{F})$  of 147.6 G is within the overall spread of computed values obtained with four different basis sets, the latter ranging from 134.1 to 142.5 G using the B3LYP density functional method and from 141.0 to 152.0 G with the MP2 method. Second, the absolute  $a(^{13}\text{C})$  value of 5.2 G determined from the  $c\text{-}^{13}\text{C}_4\text{F}_8^{\bullet-}$  spectrum is similarly in accord with the small values calculated by both the B3LYP and MP2 methods for which the magnitudes range from 2.2 to 5.2 G and 3.4–4.1 G, respectively. This excellent concordance between the experimental and theoretical results strongly supports the assignment of  $c\text{-C}_4\text{F}_8^{\bullet-}$  to the  ${}^2A_{2u}$  ground state.

Even from a strictly empirical standpoint, this low value of  $a(^{13}\text{C})$  is significant since it is found to be characteristic of  $\pi$ -type radicals or radical ions for which the SOMO possesses a nodal plane at the carbon atoms.<sup>54</sup> The nodal properties of the  $5a_{2u}$  orbital shown in Figure 7b clearly shows this plane extending through all four carbon atoms of  $c\text{-C}_4\text{F}_8^{\bullet-}$ . There is, of course, no direct contribution from the carbon  $2s$  orbitals to the wave function in this case, and so the small Fermi contact interaction responsible for the isotropic coupling presumably arises only indirectly from  $\pi$ - $\sigma$  and core spin-polarization effects, as discussed extensively for hydrocarbon  $\pi$  and  $\pi^*$  radicals.<sup>54</sup> In fact, for the double- $\zeta$  basis sets the contribution of C basis functions to  $5a_2''$  (for  $c\text{-C}_3\text{F}_6^{\bullet-}$ ) and  $5a_{2u}$  (for  $c\text{-C}_4\text{F}_8^{\bullet-}$ ) natural orbitals is exclusively  $p_z$ ,  $d_{xz}$ , and  $d_{yz}$ -type atomic orbitals. Although the parallel between  $c\text{-C}_4\text{F}_8^{\bullet-}$  and the prototype  $\text{CH}_3^{\bullet}$  ( $\pi$ ) and  $\text{C}_6\text{H}_6^{\bullet-}$  ( $\pi^*$ ) radicals rests only on this nodal character, the  $a(^{13}\text{C})$  values are found to be roughly comparable when normalized to the same number of spin-bearing carbons. The  $a(^{13}\text{C})$  values of 38.5 and 2.8 G for  $\text{CH}_3^{\bullet}$  and  $\text{C}_6\text{H}_6^{\bullet-}$ ,<sup>54</sup> respectively, then correspond to 9.6 and 4.2 G for an equivalent four-carbon radical, and hence the  $a(^{13}\text{C})$  value of 5.2 G for  $c\text{-C}_4\text{F}_8^{\bullet-}$  can be regarded as quite typical of  $\pi$ -radical systems generally.

The diagnostic value of this  $^{13}\text{C}$  coupling also becomes evident by considering an alternate assignment to the  ${}^2A_{1g}$

- (48) Reinstra-Kiracofe, J. C.; Tschumper, G. S.; Schaefer, H. F.; Nandi, S.; Ellison, G. B. *Chem. Rev.* **2002**, *102*, 231.  
 (49) Bera, P. P.; Horny, L.; Schaefer, H. F. *J. Am. Chem. Soc.* **2004**, *126*, 6692.  
 (50) Li, Q.; Feng, X.; Xie, Y.; Schaefer, H. F. *J. Phys. Chem. A* **2004**, *108*, 7071.  
 (51) Paul, A.; Wannere, C. S.; Schaefer, H. F. *J. Phys. Chem. A* **2004**, *108*, 9428.  
 (52) Xie, Y.; Schaefer, H. F.; Cotton, F. A. *Chem. Commun.* **2003**, 102.  
 (53) King, R. A.; Pettigrew, N. D.; Schaefer, H. F. *J. Chem. Phys.* **1997**, *107*, 8536.  
 (54) Gerson, F.; Huber, W. *Electron Spin Resonance Spectroscopy of Organic Radicals*; Wiley-VCH: Weinheim, Germany, 2003.

ground state. In particular, Liebman<sup>29</sup> has argued that the ordering of the  $\sigma^*$  and  $\pi^*$  antibonding molecular orbitals in the four-electron neutral  $>\text{CF}_2$  fragment is likely to be determined by the number of nodes between the atoms. According to this criterion, the  $\sigma^*$  orbital is of lower energy than the  $\pi^*$  orbital, and consequently he has suggested<sup>29</sup> that electron attachment by  $-(\text{CF}_2)_n-$  for  $n = 4$  takes place into a totally symmetric  $a_{1g}$  (local  $\sigma^*$ ) orbital rather than an  $a_{2u}$  (local  $\pi^*$ ) orbital. However, an  $a_{1g}$  SOMO would be expected to have large coefficients from the carbon 2s atomic orbitals leading to a substantial  $^{13}\text{C}$  coupling. Using the benchmark  $a(^{13}\text{C})$  value of 271.6 G for the pyramidal  $\text{CF}_3^{\bullet}$  radical<sup>33</sup> as illustrative of a SOMO with a large carbon 2s coefficient,<sup>55</sup> a conservative estimate of the  $^{13}\text{C}$  coupling for a  $^2A_{1g}$  ground state of  $c\text{-C}_4\text{F}_8^{\bullet-}$  could be as high as ca. 270 G/4 or 60–80 G. Therefore, in a choice between the  $^2A_{1g}$  and  $^2A_{2u}$  states, the finding of the much lower  $a(^{13}\text{C})$  value of 5.2 G for  $c\text{-C}_4\text{F}_8^{\bullet-}$  strongly discriminates in favor of the  $^2A_{2u}$  state, in agreement with the theoretical calculations predicting that the latter is indeed the lower energy (ground) state.

It is useful to inquire further into the reason Liebman's heuristic analysis<sup>29</sup> fails to predict the correct SOMO for  $c\text{-C}_4\text{F}_8^{\bullet-}$ , especially since he presents two additional arguments that strongly favor electron occupation into the  $\sigma^*$  over the  $\pi^*$  orbital of the localized  $>\text{CF}_2$  fragment.<sup>56</sup> First, he points out<sup>29</sup> that each  $>\text{CF}_2$  fragment is isoelectronic with  $\text{PF}_4^{\bullet}$  and other nine valence-electron radicals which are in fact known to be  $\sigma^*$  radicals with a large 2s contribution to the SOMO from the central atom.<sup>57–59</sup> Second, since the local  $\sigma^*$  orbital of each  $>\text{CF}_2$  fragment is C–F antibonding and F–F bonding, whereas the  $\pi^*$  orbital is both C–F and F–F antibonding, it is argued<sup>29</sup> that their energies are again expected to be in the order  $\sigma^* < \pi^*$ . Such considerations, however, apply only to the orbitals of the  $>\text{CF}_2$  fragments and fail to take into account the strong C–C bonding that occurs with the overlapping of the local  $\pi^*$  orbitals to form the singly occupied  $a_{2u}$  orbital in  $c\text{-C}_4\text{F}_8^{\bullet-}$ , as is shown clearly by the representation of the nodal surfaces in Figure 7. In sharp contrast, the equatorial components of the local  $\sigma^*$  orbitals are directed away from the cyclobutane ring in forming the  $a_{1g}$  orbital in  $c\text{-C}_4\text{F}_8^{\bullet-}$ , so that there is little overlap in this case between adjacent carbons. This preferential lowering of the  $a_{2u}$  orbital energy through strong C–C  $\pi^*$  overlap therefore explains this apparent reversal in the  $\sigma^*$  and  $\pi^*$  orbital ordering in going from a single  $>\text{CF}_2$  fragment to  $c\text{-C}_4\text{F}_8^{\bullet-}$ . The effect is directly attributable to the carbon connectivity but is further reinforced by the cyclic  $D_{4h}$  geometry of the  $c\text{-C}_4\text{F}_8^{\bullet-}$  anion. Parallel considerations clearly apply to  $c\text{-C}_3\text{F}_6^{\bullet-}$  and  $c\text{-C}_5\text{F}_{10}^{\bullet-}$ .

Since this paper was submitted, a recent theoretical study of electron capture by linear-chain perfluoroalkanes has come to our attention in which the odd electron is predicted to be largely concentrated in a single C–F antibonding orbital with a consequent reduction in symmetry relative to the neutral

molecule.<sup>51</sup> For example, in the negative ion of  $\text{C}_3\text{F}_8$ , the spin concentrates in just one of the two C–F antibonding orbitals of the central carbon. The only significant sharing of the spin density with other C–F bond orbitals is via a trans effect to the bonds on adjacent (beta) carbons (as depicted in Figure 6 of ref 51). This trend for linear-chain perfluoroalkanes is in remarkable contrast to the  $c\text{-C}_n\text{F}_{2n}^{\bullet-}$  analogues where the odd electron is now C–F antibonding with all the C–F bonds being equivalent and the molecular symmetry is either maintained ( $n = 3$ ) or even increased ( $n = 4$ ) on electron capture.

Due to similarities between these perfluorocycloalkane radical anions and hypervalent radicals in which a central atom bears nine electrons, a final comment on the “hypervalent” character of these  $c\text{-C}_n\text{F}_{2n}^{\bullet-}$  species is appropriate. A hypervalent molecule is generally defined as one that contains a main-group element formally bearing more than eight electrons in its valence shell.<sup>60,61</sup> The concept of an increased valence traditionally derives from valence-shell expansion through the use of d-orbitals, but it is also understandable in terms of MO theory without d-orbital participation.<sup>62–64</sup> This latter description has been applied to hypervalent radicals with nine electrons around a central atom, where the odd electron formally assumes the stereochemical role of a phantom ligand, as exemplified by the phosphoranyl radicals,  $\text{POCl}_3^{\bullet-}$ ,<sup>57</sup>  $\text{PH}_4^{\bullet}$ ,<sup>58</sup> and  $\text{PF}_4^{\bullet}$ .<sup>59</sup> These species can be considered to adopt a trigonal bipyramidal geometry such that the odd electron is formally assigned to an equatorial  $\sigma^*$  orbital on the pentacoordinate phosphorus atom.<sup>65</sup> In the case of the  $c\text{-C}_n\text{F}_{2n}$  negative ions, however, the odd electron occupies a  $\pi^*$ -type orbital at each  $>\text{CF}_2$  group, and there is essentially no equatorial  $\sigma^*$  contribution to the spin population on the carbons (vide supra). Accordingly, a hypervalent description couched in valence-bond terminology is incapable of explaining the electronic structure of the  $c\text{-C}_n\text{F}_{2n}$  negative ions, and the hypervalency of these species is best regarded as exemplar of the occupation of antibonding orbitals in saturated molecules, similar at least in principle to the description of the prototype excess-electron molecule  $\text{F}_2^{\bullet-}$ .<sup>66–69</sup>

## 7. Conclusions

The experimental and theoretical data strongly support the following assignments for the ground electronic states (and point group symmetries) of the three anions:  $c\text{-C}_3\text{F}_6^{\bullet-}$ ,  $^2A_2'' (D_{3h})$ ;  $c\text{-C}_4\text{F}_8^{\bullet-}$ ,  $^2A_{2u} (D_{4h})$ ; and  $c\text{-C}_5\text{F}_{10}^{\bullet-}$ ,  $^2A' (C_s)$ . Although the equilibrium structure of  $c\text{-C}_5\text{F}_{10}^{\bullet-}$  belongs to the  $C_s$  point group, computations suggest that a process interconverting the 5 equivalent puckered conformations readily occurs which leads to the observation that, in the ESR spectrum, all 10 fluorines

(55) Since the  $a(^{13}\text{C})$  value of 271.6 G corresponds to a 2s spin density of ca. 0.25, the unpaired electron in the  $\text{CF}_3^{\bullet}$  radical can, to a good approximation, be considered to occupy a carbon-centered  $\text{sp}^3$  orbital.

(56) For the sake of clarity, it should be noted that both the  $\sigma^*$  and  $\pi^*$  localized  $>\text{CF}_2$  orbitals (Liebman's notation) include contributions from the C–F  $\sigma^*$  orbitals.

(57) Gillbro, T.; Williams, F. *J. Am. Chem. Soc.* **1974**, *96*, 5032.

(58) Colussi, A. J.; Morton, J. R.; Preston, K. F. *J. Phys. Chem.* **1975**, *79*, 1855.

(59) Hasegawa, A.; Ohnishi, K.; Sogabe, K.; Miura, M. *Mol. Phys.* **1975**, *30*, 1367.

(60) Musher, J. I. *Angew. Chem., Int. Ed. Engl.* **1969**, *8*, 54.

(61) Akiba, K., Ed.; *Chemistry of Hypervalent Compounds*; Wiley: New York, 1998.

(62) Rundle, R. E. *J. Am. Chem. Soc.* **1963**, *85*, 112.

(63) Rundle, R. E. *Surv. Prog. Chem.* **1963**, *1*, 81.

(64) Hoffmann, R.; Howell, J. H.; Mutterties, E. L. *J. Am. Chem. Soc.* **1972**, *94*, 3047.

(65) It should be added that this representation of these phosphoranyl radicals is only an approximate description since both experimental results<sup>57–59</sup> and MO calculations (Howell, J. M.; Olsen, J. F. *J. Am. Chem. Soc.* **1976**, *98*, 7119) find that almost half the total spin density resides in the bonding orbitals of the axial ligands. For ab initio theoretical studies of phosphoranyl radicals, see: Gustafson, S. M.; Cramer, C. J. *J. Phys. Chem.* **1995**, *99*, 2267 and references therein.

(66) Castner, T. G.; Känzig, W. *J. Phys. Chem. Solids* **1957**, *3*, 178.

(67) Delbecq, C. J.; Hayes, W.; Yuster, P. H. *Phys. Rev.* **1961**, *121*, 1043.

(68) Gazzinelli, R.; Mieher, R. *Phys. Rev. Lett.* **1964**, *12*, 644.

(69) McCorkle, D. L.; Christophorou, L. G.; Christodoulides, A. A.; Pichiarella, L. *J. Chem. Phys.* **1986**, *85*, 1966.

have the same  $^{19}\text{F}$  hyperfine coupling corresponding to the average environment of the F atoms.

Two of the closed-shell neutral species also adopt highly symmetric equilibrium structures. The *c*- $\text{C}_3\text{F}_6$  molecule adopts the same geometry as its anion ( $D_{3h}$ ), and *c*- $\text{C}_4\text{F}_8$  has a puckered  $D_{2d}$  geometry. However, the *c*- $\text{C}_5\text{F}_{10}$  molecule is tentatively assigned a  $C_1$  equilibrium structure that deviates slightly from  $C_s$  symmetry.

Although the computed adiabatic electron affinities vary widely with the method and basis set used (by as much 0.5 eV), three remarkably consistent trends are clear. (1) *c*- $\text{C}_4\text{F}_8$  and *c*- $\text{C}_5\text{F}_{10}$  have nearly identical AEAs (within  $\sim 0.1$  eV). (2) The AEA of *c*- $\text{C}_3\text{F}_6$  is approximately half that of *c*- $\text{C}_4\text{F}_8$  and *c*- $\text{C}_5\text{F}_{10}$ . (3) The ZPVE correction increases all of the AEAs by  $\sim 0.17$  eV.

**Acknowledgment.** The authors at the University of Mississippi would like to thank the Mississippi Center for Supercomputing Research for generous amounts of CPU time. A.M.E. would like to thank Brian W. Hopkins for helpful discussions throughout the project. G.S.T. is supported in part by the

National Science Foundation (EPS-0132618) and by the Research Corporation (RI 1089). The research at the University of Tennessee was supported by the Division of Chemical Sciences, Office of Basic Energy Sciences, United States Department of Energy under Grant No. DE-FG02-88ER13852 to F.W. The Tennessee authors also wish to acknowledge the gift of a perfluorocyclopropane sample from Professor Richard W. Fessenden, the interest and encouragement of the late Professor Gleb Mamantov in the early stages of this project, the experimental assistance afforded by Stephen Dorris in the ESR work, and the contribution of Rick Cook in Professor John Z. Larese's group for scanning the ESR spectral images into JPEG files.

**Supporting Information Available:** Experimental details, computational details, and Cartesian coordinates of optimized structures. This material is available free of charge via the Internet at <http://pubs.acs.org>.

JA0505898